

## MAPPING THE DARK MATTER WITH POLARIZED RADIO SURVEYS

MICHAEL L. BROWN<sup>1,2</sup> AND RICHARD A. BATTYE<sup>3</sup>

<sup>1</sup>Astrophysics Group, Cavendish Laboratory, University of Cambridge, J J Thomson Avenue, Cambridge CB3 0HE, United Kingdom

<sup>2</sup>Kavli Institute for Cosmology, University of Cambridge, Madingley Road, Cambridge CB3 0HA, United Kingdom

<sup>3</sup>Jodrell Bank Centre for Astrophysics, School of Physics and Astronomy, University of Manchester, Oxford Road, Manchester, M13 9PL, United Kingdom

*Draft version June 15, 2022*

### ABSTRACT

In a recent paper (Brown & Battye 2011), we proposed the use of integrated polarization measurements of background galaxies in radio weak gravitational lensing surveys and investigated the potential impact on the statistical measurement of cosmic shear. Here we extend this idea to reconstruct maps of the projected dark matter distribution, or lensing convergence field. The addition of polarization can, in principle, greatly reduce shape noise due to the intrinsic dispersion in galaxy ellipticities. We show that maps reconstructed using this technique in the radio band can be competitive with those derived using standard lensing techniques which make use of many more galaxies. In addition, since the reconstruction noise is uncorrelated between these standard techniques and the polarization technique, their comparison can serve as a powerful check for systematics and their combination can reduce noise further. We examine the convergence reconstruction which could be achieved with two forthcoming facilities: (i) a deep survey, covering  $1.75 \text{ deg}^2$  using the e-MERLIN instrument currently being commissioned in the UK and (ii) the high resolution, deep wide field surveys which will eventually be conducted with the Square Kilometre Array (SKA).

*Subject headings:* cosmology: theory – dark matter, gravitational lensing: weak, radio continuum: galaxies, polarization

### 1. INTRODUCTION

Weak gravitational lensing has become one of the most powerful techniques for investigating the distribution of dark matter on cosmological scales (e.g. Massey et al. 2007; Heymans et al. 2008; Schrabback et al. 2010). The majority of weak lensing studies to date have been conducted in the optical bands since large numbers of galaxies are required to reduce the shape noise associated with the intrinsic ellipticities of galaxies. Observationally, the pace of progress in the optical is set to continue with forthcoming wide-field surveys using a number of purpose-built instruments, e.g. DES<sup>1</sup>, KIDS<sup>2</sup>, Euclid<sup>3</sup>, WFIRST<sup>4</sup> and Pan-STARRS<sup>5</sup>.

As the statistical precision of optical surveys improves, greater control over potential systematics is required. Major systematics of concern include instrumental effects such as anisotropies in the point-spread function (PSF) of the telescope and astrophysical systematics such as intrinsic galaxy alignments (e.g. Crittenden et al. 2001; Catelan et al. 2001; Hirata & Seljak 2004).

In addition to a new generation of wide-field optical surveys, a suite of powerful next-generation radio instruments are due to come online in the near future. Radio instruments offer a number of potential advantages over optical surveys for lensing studies. In particular, radio interferometers do not suffer from complicated PSF effects, their synthesized beams being precisely and solely determined by the telescope array configuration and direction of observation.

A further unique advantage offered by measuring lensing in the radio band is the polarization information which is usually measured in addition to the total intensity in radio surveys.

Previous authors have exploited the fact that the polarization position angle is unaffected by lensing in order to measure gravitational lensing of distant quasars (Kronberg et al. 1991, 1996; Burns et al. 2004). In a recent paper (Brown & Battye 2011), we showed how one could extend this idea to measure cosmic shear. The technique relies on there existing a reasonably tight relationship between the orientation of the integrated polarized emission and the intrinsic morphological orientation of the galaxy. The existence of this relationship needs to be established for the high-redshift star-forming galaxies which are expected to dominate the radio sky at the  $\mu\text{Jy}$  flux sensitivities achievable with forthcoming instruments. However, such a relationship certainly exists in the local Universe (Stil et al. 2009) and it is reasonable to assume that it persists to higher redshift.

A key difference between the polarization technique and standard techniques for measuring lensing is that the former *does not* assume that the ensemble average of the intrinsic shapes of galaxies vanishes. It is thus, in principle, able to cleanly discriminate between a lensing signal and a possible contaminating signal due to intrinsic galaxy alignments (Brown & Battye 2011).

In this letter, we investigate the direct reconstruction of the projected dark matter distribution (or lensing convergence field) using the radio polarization technique. Our simulations are based on the ray-tracing simulations of White (2005). We begin in Section 2 by summarizing the salient features of these simulations and we describe the parameters we have adopted to mimic the e-MERLIN<sup>6</sup> (currently being commissioned with full operation planned for the second half of 2011) and SKA<sup>7</sup> instruments. In Section 3, we describe how to include polarization information in a direct-inversion mass reconstruction algorithm and we present our simulation results.

<sup>1</sup> <http://www.darkenergysurvey.org>

<sup>2</sup> <http://www.strw.leidenuniv.nl/~kuijken/KIDS/>

<sup>3</sup> <http://sci.esa.int/science-e/www/area/index.cfm?fareaid=102>

<sup>4</sup> <http://wfirst.gsfc.nasa.gov/>

<sup>5</sup> <http://pan-starrs.ifa.hawaii.edu>

<sup>6</sup> <http://www.e-merlin.ac.uk>

<sup>7</sup> <http://www.skatelescope.org>

We finish in Section 4 with a discussion.

## 2. SIMULATIONS

To demonstrate the mass reconstruction technique using polarization information, we have made use of the simulated lensing convergence and shear maps of White (2005)<sup>8</sup>. These simulations comprise  $\approx 1000$  square degrees of simulated sky from high resolution numerical simulations based on a  $\Lambda$ CDM cosmology with parameters,  $\Omega_m = 0.28, \Omega_b h^2 = 0.024, h = 0.7, \sigma_8 = 0.9$  and  $n_s = 1$ . The simulations consist of 112  $3 \times 3 \text{ deg}^2$  fields which are approximately independent.

The assumed redshift distribution is of the form,  $n(z) \propto z^2 \exp(-z/z_0)^\beta$  with  $z_0 = 1.0$  and  $\beta = 1.5$ . The median redshift of this distribution is  $z_m = 1.41$ . Making use of the semi-empirical SKA Design Studies (SKADS) simulation of Wilman et al. (2008)<sup>9</sup>, we have checked that this  $n(z)$  agrees reasonably well with the redshift distribution of star-forming galaxies expected in future deep radio surveys. In particular, we measure  $z_m = 1.02$  in the SKADS simulation for a  $10\sigma$  detection threshold of  $40 \mu\text{Jy}$ , a sensitivity which could be reached over  $1.75 \text{ deg}^2$  using e-MERLIN. Large-scale surveys with the SKA might go  $\sim 10$  times deeper (e.g. Blake et al. 2007). At this depth, we measure a median redshift of  $z_m = 1.48$  from the SKADS simulation. Although the predicted median redshift of the proposed e-MERLIN survey is somewhat smaller than that of White’s simulations, this discrepancy is sub-dominant when compared to the current very large uncertainties in predicting  $n(z)$  for  $\mu\text{Jy}$ -sensitivity radio surveys.

A further unknown for forthcoming radio surveys is the number density of galaxies that will be achieved. Source counts at 1.4 GHz are presented in Biggs & Ivison (2006) for deep fields over relatively small areas of sky. Extrapolating from this study suggests a source density of  $\sim 1 \text{ arcmin}^{-2}$  for a detection threshold of  $40 \mu\text{Jy}$ . This source density is also consistent with that found in deep VLA + MERLIN observations of the Hubble Deep Field (Muxlow et al. 2005). The source counts from a more recent study by Owen & Morrison (2008) are significantly higher and suggest a source density of  $2 \text{ arcmin}^{-2}$  could be achieved. For the e-MERLIN simulations, we take the average of these two estimates and adopt  $\bar{n} = 1.5 \text{ arcmin}^{-2}$  for the number density of galaxies detected in total intensity. For the SKA simulations, we assume  $\bar{n} = 15 \text{ arcmin}^{-2}$ .

The polarization properties of the high-redshift star-forming galaxies which will dominate these surveys are currently unknown. We can only extrapolate from the local Universe where the fractional polarization is typically between 0 and 20% (Stil et al. 2009). These observations of local galaxies also suggest that the polarized emission and the morphological orientation are well aligned to an accuracy of between 0 and  $\sim 15$  degs.

For our simulations, we assume that the galaxies are, on average, 10% polarized. Noting that a measurement of the orientation of the polarized emission requires only a third of the sensitivity which would be required to measure the shape of the emission, we assume further that we can measure a useful polarization orientation for one third of the galaxies detected in total intensity. Thus, we assume  $\bar{n}_{\text{pol}} = 0.5 \text{ arcmin}^{-2}$  for e-MERLIN and  $\bar{n}_{\text{pol}} = 5.0 \text{ arcmin}^{-2}$  for the SKA. We fur-

ther assume that such polarization orientation detections are an unbiased tracer of the intrinsic morphological orientation of the galaxy with a scatter of  $\alpha_{\text{rms}} = 7$  degs. (See Section 2 of Brown & Battye 2011 for further discussion on the current observational status for polarization and possible values for these parameters.)

To mimic the proposed e-MERLIN survey, we extract the central  $1.75 \text{ deg}^2$  from each  $3 \times 3 \text{ deg}^2$  simulation. An example of the convergence distribution for one field is shown in the top left panel of Fig. 1 where a number of large-scale structures and filaments are clearly visible. Using the parameters detailed above, we generate background galaxies randomly distributed across the field of view. Each galaxy is assigned an intrinsic ellipticity,  $\epsilon = \epsilon_1 + i\epsilon_2$  where  $\epsilon_1$  and  $\epsilon_2$  are drawn from zero-mean Gaussian distributions with width  $\sigma_\epsilon = 0.30$ . For each galaxy, we then add the simulated shear to the intrinsic ellipticity, interpolating the shear from the numerical simulations.

For the polarization technique, we additionally simulate the observed orientation of the polarized emission of each galaxy according to  $\alpha^{\text{obs}} = \alpha^{\text{int}} + \alpha^{\text{rand}}$  where  $\alpha^{\text{int}} = (1/2) \tan^{-1}(\epsilon_2/\epsilon_1)$  is the intrinsic position angle of the galaxy and  $\alpha^{\text{rand}}$  is the random noise in the polarized orientation—intrinsic position angle relationship.

## 3. MASS RECONSTRUCTION USING POLARIZATION

To reconstruct the convergence field from the simulated galaxy catalogues, we use a variant of the Kaiser-Squires direct-inversion technique (Kaiser & Squires 1993). Our implementation is similar to the real-space algorithm described in Seitz & Schneider (1995). To perform the reconstruction using the total intensity only (i.e. using the standard lensing technique), following Seitz & Schneider (1995), we first estimate the mean shear field on a regular grid covering the entire field. We estimate the shear in each grid cell as (the indexes,  $\{i, j\}$  denote the grid cells)

$$\hat{\gamma}_{i,j} = \frac{\sum_k w_k \epsilon_k^{\text{obs}}}{\sum_k w_k} \quad (1)$$

where the sum is over all galaxies and we have applied a weight of

$$w_k = \exp\left(-\frac{(\theta_{i,j} - \theta_k)^2}{(\Delta\theta)^2}\right) \quad (2)$$

to each of the observed ellipticities,  $\epsilon_k^{\text{obs}}$ . We use a smoothing scale of  $\Delta\theta = 2.0 \text{ arcmin}$ . The convergence field is then estimated as a convolution,

$$\hat{\kappa}(\theta) = -\frac{1}{2\pi} \sum_{i,j} \text{Re}[\mathcal{D}(\theta - \theta_{i,j}) \gamma^*(\theta_{i,j})] \quad (3)$$

where the kernel,  $\mathcal{D}$  is given by

$$\mathcal{D} = \frac{\theta_1^2 - \theta_2^2 + 2i\theta_1\theta_2}{|\theta|^4} \quad (4)$$

Including the polarization information in this estimator is straightforward and simply involves using a weighted version of the shear estimator described in Brown & Battye (2011) to estimate the shear at each grid point. Explicitly, the shear in each grid cell is now estimated as

$$\hat{\gamma} = \mathbf{A}^{-1} \mathbf{b}, \quad (5)$$

<sup>8</sup> Available at <http://mwhite.berkeley.edu/Lensing/Thousand/>

<sup>9</sup> See <http://s-cubed.physics.ox.ac.uk/>

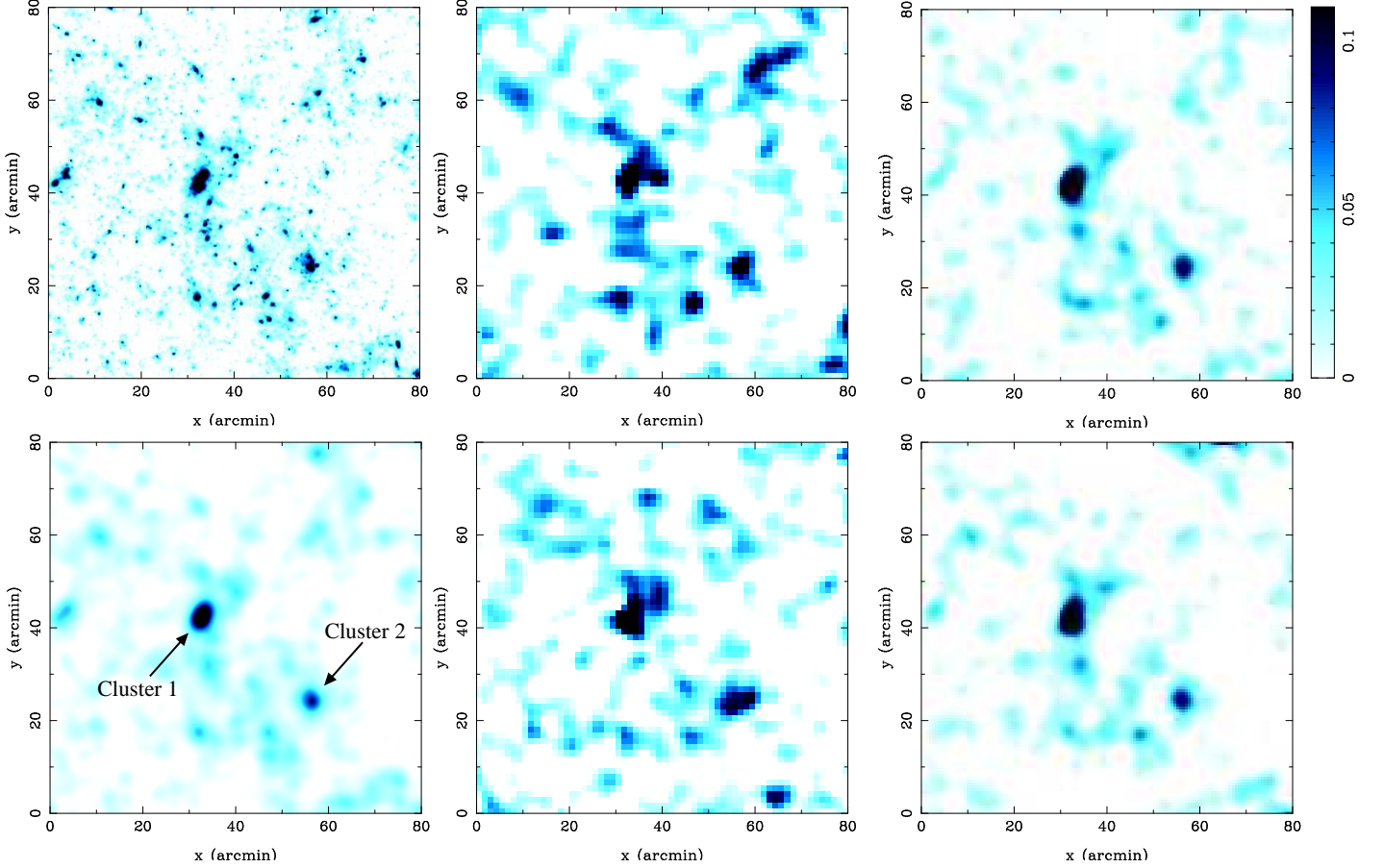


**Figure 1.** An example reconstruction of the dark matter distribution in a  $1.75 \text{ deg}^2$  region of the simulations. The input convergence field is shown unaltered in the upper left panel and smoothed with a 2 arcmin Gaussian kernel in the lower left panel. The simulated reconstruction using total intensity only for observational specifications similar to the proposed e-MERLIN survey (with  $\bar{n} = 1.5 \text{ arcmin}^{-2}$  and  $\epsilon_{\text{rms}} = 0.30$ ) is shown in the upper central panel. Assuming one third of these galaxies are sufficiently polarized to yield an intrinsic position angle tracer that is unbiased with a scatter of  $\alpha_{\text{rms}} = 7.0$  degs, the reconstruction obtained using polarization information is shown in the lower central panel. The reconstructions obtainable with the SKA are shown in the right-hand panels (upper panel — using total intensity only; lower panel — with polarization). For the SKA reconstructions, we have assumed  $\bar{n} = 15 \text{ arcmin}^{-2}$  and that one third of the galaxies are useable in polarization with  $\alpha_{\text{rms}} = 7.0$  degs. Integrated convergence measurements for the two structures labelled “Cluster 1” and “Cluster 2” are given in Table 1.

where the matrix,  $\mathbf{A}$ , and the vector,  $\mathbf{b}$ , are given by

$$\mathbf{A} = \sum_k w_k \hat{\mathbf{n}}_k \hat{\mathbf{n}}_k^T, \quad (6)$$

$$\mathbf{b} = \sum_k w_k (\epsilon_k^{\text{obs}} \cdot \hat{\mathbf{n}}_k) \hat{\mathbf{n}}_k. \quad (7)$$

Here,  $\hat{\mathbf{n}}_k = (\sin 2\alpha_k^{\text{obs}}, -\cos 2\alpha_k^{\text{obs}})$  is the direction at  $45^\circ$  to the estimate of the intrinsic position angle of the galaxy as provided by the polarization and  $w_k$  is a weight.

Using a weighting scheme in equation (5) is now crucial — the small galaxy number density we are dealing with means that “shot noise” is a severe problem for the polarization estimator.<sup>10</sup> Had we used an unweighted shear estimator (i.e. simple binning) then a significant fraction of our grid cells would contain no galaxies for the polarization estimator and this would present problems for the convolution operation. By using weights which are non-negligible at the typical separation of polarized galaxies, we can recover the shear at each point in the grid, albeit at the expense of a smoothing of the

<sup>10</sup> We discriminate here between “shape noise” which is the dispersion in the intrinsic shapes of galaxies and “shot noise” which is the noise introduced due to the finite number of galaxies and hence the sparse sampling of the underlying shear field.

shear field. In practice, we use the same weighting scheme as for the standard case (equation 2) with the same smoothing scale,  $\Delta\theta = 2.0$  arcmin, in all cases. Once the shear field has been estimated, the convergence,  $\kappa(\boldsymbol{\theta})$  is found as in the standard case (equation 3).

An example of the mass reconstruction performance for both the standard estimator and the polarization estimator is shown in Fig. 1. The simulated e-MERLIN reconstructions have been performed on a  $64 \times 64$  grid of 1.25 arcmin pixels. For the much higher fidelity SKA simulations, we use a  $128 \times 128$  grid of 0.625 arcmin pixels. We see that the major mass concentrations can be successfully identified in the simulated e-MERLIN reconstructions while the SKA maps also trace the filamentary structure of the numerical simulations extremely well. For the observational parameters we have adopted, the reconstructions obtained using the polarization estimator are of similar sensitivity to those obtained using the standard estimator. In Table 1 we list the reconstructed convergence field integrated in apertures of radius 3 arcmin for the two largest structures in the field, centred on  $(x, y) = (32.6, 42.8)$  arcmin and  $(x, y) = (56.5, 24.3)$  arcmin. The errors are determined by repeating the analysis on empty fields and measuring the root-mean-square convergence field integrated in identical apertures.

**Table 1**  
Integrated convergence measurements for the structures  
labelled “Cluster 1” and “Cluster 2” in Fig. 1.

Simulation	Standard estimator	Polarization estimator
e-MERLIN:		
Cluster 1	$2.36 \pm 0.19$	$2.31 \pm 0.18$
Cluster 2	$1.26 \pm 0.19$	$1.30 \pm 0.18$
SKA:		
Cluster 1	$2.29 \pm 0.08$	$2.13 \pm 0.07$
Cluster 2	$0.92 \pm 0.08$	$0.98 \pm 0.07$

We have also measured the shear correlation functions from the simulated maps. The correlation functions are defined as

$$\begin{aligned} C_1(\boldsymbol{\theta}) &= \langle \gamma_1^r(\boldsymbol{\theta}) \gamma_1^r(\boldsymbol{\theta} + \Delta\boldsymbol{\theta}) \rangle \\ C_2(\boldsymbol{\theta}) &= \langle \gamma_2^r(\boldsymbol{\theta}) \gamma_2^r(\boldsymbol{\theta} + \Delta\boldsymbol{\theta}) \rangle \\ C_3(\boldsymbol{\theta}) &= \langle \gamma_1^r(\boldsymbol{\theta}) \gamma_2^r(\boldsymbol{\theta} + \Delta\boldsymbol{\theta}) \rangle \end{aligned} \quad (8)$$

where the angled brackets denote an average over all map-pixel pairs separated by  $\Delta\boldsymbol{\theta}$  and  $\gamma_1^r$  and  $\gamma_2^r$  are the estimated shear components rotated to a coordinate system aligned with the vector joining the two map-pixels. The cross-correlation,  $C_3(\boldsymbol{\theta})$  is expected to vanish in the absence of parity-violating effects.

We have measured the total correlation function,  $C(\boldsymbol{\theta}) = C_1(\boldsymbol{\theta}) + C_2(\boldsymbol{\theta})$  using both the standard and polarization estimator and have also combined the results from the two techniques. Note that the combination of the two estimators is powerful since the dominant source of measurement noise is different in the two cases — for the standard estimator, the shape noise dominates while for the polarization estimator the noise associated with  $\alpha_{\text{rms}}$  dominates meaning that there is useful extra information in the cross-correlation of the shear fields estimated using the two techniques. The cross-correlation can also be useful in mitigating systematics which would likely be different for the two techniques.

The results, averaged over simulations, are plotted in Fig. 2. Naively, it looks as though a detection of cosmic shear is possible with the proposed  $1.75 \text{ deg}^2$  e-MERLIN survey. However, the measurements on different scales are strongly correlated and the formal detection significance is only  $1.4\sigma$ . Note that the dominant contribution to the errors is sample variance. Instead of doing cosmology, if we ask the question how well can we measure the lensing signal in a typical  $1.75 \text{ deg}^2$  field, then the significance is much larger ( $\sim 6.6\sigma$ ).

#### 4. DISCUSSION

In this letter, we have extended the techniques of Brown & Battye (2011) to the lensing reconstruction of dark matter maps from polarized radio surveys. For the parameters which we have adopted, the technique looks extremely promising and could make future radio surveys as powerful as optical lensing surveys containing many more galaxies.

There is, of course, a great deal of uncertainty with respect to the values one should adopt for the polarization properties of star-forming galaxies at  $\mu\text{Jy}$  flux densities. In particular, the typical fractional polarization and the degree to which the orientation of the polarized emission is aligned with the intrinsic morphological orientation are currently unknown. We note also however that there is a trade-off in these two parameters. For example, one can imagine including a larger number

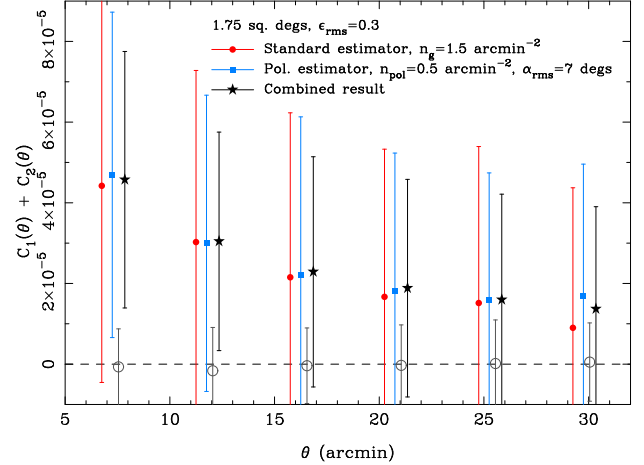


**Figure 2.** The total shear correlation function measured from the e-MERLIN simulations. Three sets of points are plotted. From left to right they have been obtained using the standard shear estimator, using the polarization estimator and their combination. The points plotted as open circles show the cross-correlation,  $C_3(\boldsymbol{\theta})$ , which is consistent with zero. Comparison of the errors on this latter measurement with those on the measurement of the signal gives an indication of the relative sizes of the measurement noise and sample variance contributions. The errors plotted are those appropriate for a single realization. Measurements on different scales are heavily correlated and the significance of the detection of cosmic shear is in fact only  $1.4\sigma$ .

of galaxies whose polarized emission and intrinsic orientation are poorly aligned (large  $\bar{n}_{\text{pol}}$  and large  $\alpha_{\text{rms}}$ ) or one could be very selective about which galaxies one includes, choosing high fractional polarization objects whose polarization orientation closely traces the major axis of the galaxy (low  $\bar{n}_{\text{pol}}$  and low  $\alpha_{\text{rms}}$ ).

In terms of forecasting constraints for future surveys, Kaiser (1998) has shown that the errors obtainable on the shear power spectrum with a survey covering a fraction of sky  $f_{\text{sky}}$  and with a galaxy number density  $\bar{n}$  are given by

$$\Delta C_\ell = \sqrt{\frac{2}{(2\ell+1)f_{\text{sky}}}} \left( C_\ell + \frac{\epsilon_{\text{rms}}^2}{\bar{n}} \right). \quad (9)$$

The equivalent expression for the polarization case is

$$\Delta C_\ell = \sqrt{\frac{2}{(2\ell+1)f_{\text{sky}}}} \left( C_\ell + \frac{16\alpha_{\text{rms}}^2 \epsilon_{\text{rms}}^2}{\bar{n}_{\text{pol}}} \right). \quad (10)$$

In Fig. 3, we have plotted these predictions for some representative numbers chosen to mimic large-scale surveys to be conducted with the SKA. If the polarization properties of star-forming galaxies assumed here turn out to be reasonable, then it will be very interesting to apply the polarization techniques described here and elsewhere to forthcoming high-resolution  $\mu\text{Jy}$ -sensitivity radio surveys.

#### REFERENCES

- Biggs, A. D. & Ivison, R. J. 2006, MNRAS, 371, 963  
 Blake C., Bacon D., Fluke C., Kitching T., Miller L., Power C., Wilman R., 2007, SKADS Virtual Telescope Proposal, available at <http://www.skads-eu.org/p/svt/svt2007.php>  
 Brown, M. L. & Battye, R. A. 2011, MNRAS, 410, 2057  
 Burns C. R., Dyer C. C., Kronberg P. P., Röser H., 2004, ApJ, 613, 672  
 Catelan P., Kamionkowski M., Blandford R. D., 2001, MNRAS, 320, L7  
 Crittenden R. G., Natarajan P., Pen U., Theuns T., 2001, ApJ, 559, 552

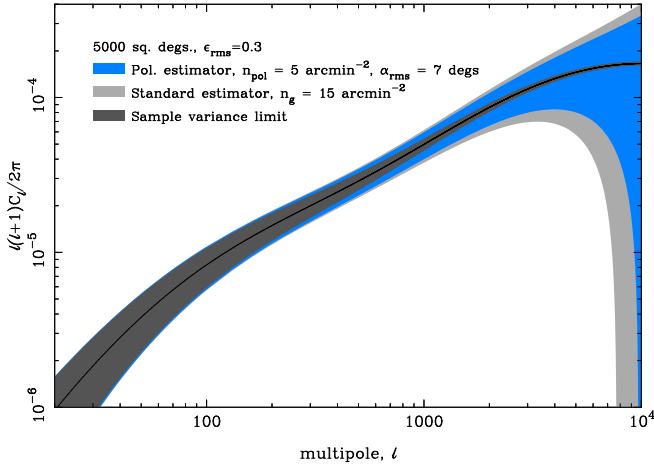


**Figure 3.** Predicted per-multipole uncertainties on the weak lensing power spectrum for a  $5000 \text{ deg}^2$  survey with  $\bar{n} = 15 \text{ arcmin}^{-2}$  and  $\epsilon_{\text{rms}} = 0.3$ . The forecasts using the polarization estimator assume that one third of these galaxies are detected sufficiently well in polarization such that  $\alpha_{\text{rms}} = 7 \text{ degs}$ . The cosmic variance limit is also shown for comparison.

- Heymans, C. et al. 2008, MNRAS, 385, 1431  
 Hirata C. M., Seljak U., 2004, Phys. Rev. D, 70, 063526  
 Kaiser, N. 1998, ApJ, 498, 26  
 Kaiser, N. & Squires, G. 1993, ApJ, 404, 441  
 Kronberg P. P., Dyer C. C., Burbidge E. M., Junkkarinen V. T., 1991, ApJ, 367, L1  
 Kronberg P. P., Dyer C. C., Roeser H., 1996, ApJ, 472, 115  
 Massey, R. et al. 2007, Nature, 445, 286  
 Muxlow, T. W. B. et al. 2005, MNRAS, 358, 1159  
 Owen, F. N. & Morrison, G. E. 2008, AJ, 136, 1889  
 Schrabback, T. et al. 2010, A&A, 516, A63+  
 Seitz, C. & Schneider, P. 1995, A&A, 297, 287  
 Stil, J. M., Krause, M., Beck, R., & Taylor, A. R. 2009, ApJ, 693, 1392  
 White, M. 2005, Astroparticle Physics, 23, 349  
 Wilman, R. J. et al. 2008, MNRAS, 388, 1335